The influence of second phase particles on brittle fracture

E. A. ALMOND, D. H. TIMBRES and J. D. EMBURY
Department of Metallurgy and Materials Science,
McMaster University, Hamilton, Ontario

Summary
A model for slip induced cleavage fracture has been proposed which considers the equilibrium of a crack in a brittle second phase particle when it is acted upon both by the applied stress system and the stresses due to a pile up in an unrelaxed slip band. The model has been used successfully to give a quantitative explanation for experimental results for the effect of grain size and carbide size on the fracture stress of Armco iron. An examination of the fracture surfaces by scanning electron microscopy has revealed that some microstructural features such as dispersed carbides may greatly alter the topology of cleavage facets and thus increase the total surface energy required for crack propagation.

Introduction

The Petch [1] and Cottrell [2] theories for cleavage fracture recognize the importance of microstructure in determining the stress for the twinning or yielding mechanism that precedes crack formation. However these models do not consider the effect of microstructural inhomogeneities on the initiation and propagation of cleavage cracks and thus are not applicable to some steels where cleavage fracture is initiated by the fracture of grain boundary carbides [3, 4, 5]. Stroh [6] and Smith [7] have stressed crack propagation and not crack initiation is the event of controlling fracture only under conditions where the crack is initiated in regions with lower effective surface energy than the surrounding matrix. This condition is fulfilled if cleavage is initiated by the fracture of boundary carbide and the important stage is the growth of the particle sized crack into the ferrite matrix. Smith [8] examined this situation for a cleavage crack which is coplanar with the initiating slip band by using continuous distributions of dislocations to represent the local displacements parallel and perpendicular to the crack. In the present work a simple energy balance method was used to derive the condition for crack propagation and the role of carbides in the cleavage fracture of iron has been examined experimentally. In addition evidence is presented to illustrate the effects of dispersed carbides and grain boundaries on the subsequent propagation of cleavage cracks.

Proposed model

Consider a material containing rigid particles at the grain boundary. Inhomogeneous plastic deformation occurs in the form of a slip band which

impinges on the particle as shown schematically in Fig. 1. If the particle is a soft plastic inclusion the slip band may be relaxed by deformation in the particle. However, if the material is brittle a crack can be formed in the particle with an effective energy γ_p equal to the true surface energy of the particle and much less than γ the effective surface energy of a cleavage crack in the matrix. The matrix now contains a crack of length t which is acted upon both by the applied stress system and the stresses due to the pile up of dislocations in the slip band which is assumed to be unrelaxed by the failure of the particle. The crack will either be relaxed by plastic deformation in the neighbouring ferrite grain or propagate as a cleavage crack. Following the failure of the particle the wedging action of the dislocation pile up is effectively transferred to the tip of the crack and the energy considerations for extending the crack into the ferrite will be similar to those for the formation of a cracked dislocation at the tip of the pre-existing crack. The energy involved in extending the crack of length t to a length $(r + t)$ under the action of an applied normal stress p will be,

$$W = \frac{\mu n^2 a^2}{4\pi(1-\nu)} \ln\left(\frac{4L}{r}\right) + 2\gamma r - \frac{pna}{2}(r+t) + \frac{\pi(1-\nu)\, p^2 t^2}{8\mu} - \frac{\pi(1-\nu)\, p^2 (r+t)^2}{8\mu} \qquad (1)$$

where the first two terms are the energy of a cracked dislocation of strength na[9], L being the effective radius of the stress field of the dislocation and γ the effective surface energy of the ferrite; the third term is the work done by the applied stress due to the change in volume on opening up the crack, the fourth and fifth term describe the change in the elastic energy of the growing crack in the applied stress field.
Let

$$C_1 = \frac{\mu n^2 a^2}{8\pi(1-\nu)\gamma}\ ;\ C_2 = \frac{8\mu\gamma}{\pi(1-\nu)\, p^2}\ ;\ \left(\frac{C_1}{C_2}\right)^{1/2} = \frac{pna}{8\gamma}$$

then equation 1 has stationary values when

$$\frac{dW}{dr} = 2\gamma\left(-\frac{C_1}{r} - 2\left(\frac{C_1}{C_2}\right)^{1/2} + 1 - \frac{(r+t)}{C_2}\right) = 0 \qquad (2)$$

i.e. when

$$r^2 - \left(1 - 2\left(\frac{C_1}{C_2}\right)^{1/2} - \frac{t}{C_2}\right) C_2\, r + C_1 C_2 = 0 \qquad (3)$$

and has real roots (positive crack lengths) when

$$\left(1 - 2\left(\frac{C_1}{C_1}\right)^{1/2} - \frac{t}{C_2}\right)^2 C_2^2 > 4\, C_1 C_2 \qquad (4)$$

If the roots are imaginary there is no position of equilibrium and the cracks are unstable. Thus brittle behaviour is expected when

$$\left(1 - 2\left(\frac{C_1}{C_2}\right)^{1/2} - \frac{t}{C_2}\right)^2 C_2^2 < 4\, C_1 C_2$$

$$4\left(\frac{C_1}{C_2}\right)^{1/2} + \frac{t}{C_2} > 1$$

$$\frac{pna}{2\gamma} + \frac{(1-\nu)}{8\mu\gamma} p^2\, t > 1 \qquad (5)$$

Since $na = \{[\pi(1-\nu)l]/2\mu\}\,\sigma_s$ [2] where σ is effective shear stress on the pile up in a grain of diameter l and at the yield condition $\sigma_s = (kl^{-1/2})/2$ where k is the slope of the Hall-Petch equation for uniaxial tension

$$\text{then } p\sigma_s\ l + \frac{p^2 t}{2} > \frac{4\mu\gamma}{\pi(1-\nu)} \qquad (6)$$

When the carbide thickness t is zero this expression reduces to the Petch condition for crack propagation

$$p > \frac{4\mu\gamma}{\pi(1-\nu)\sigma_s l} \text{ or } p > \frac{8\mu\gamma}{\pi(1-\nu)\ kl^{1/2}} \qquad (7)$$

but for finite values of t,

$$p = \left(\frac{\sigma_s^{\,2}\, l^2}{t^2} + \frac{8\mu\gamma}{\pi(1-\nu)t}\right)^{1/2} - \frac{\sigma_s l}{t} \qquad (8)$$

and when fracture occurs at the yield stress.

$$p = \sigma_y = \left(\frac{k^2 l}{4t^2} + \frac{8\mu\gamma}{\pi(1-\nu)t}\right)^{1/2} - \frac{kl^{1/2}}{2t} \qquad (9)$$

In notch bend tests when the general yield condition is reached the maximum tensile stress is $R\sigma_y$ where R is the plastic constraint factor appropriate to the notch geometry [10]. Thus crack propagation can occur at the general yield stress under the notch when

$$R\sigma_y > \left(\frac{k^2 l}{4t^2} + \frac{8\mu\gamma}{\pi(1-\nu)t}\right)^{1/2} - \frac{kl^{1/2}}{2t} \qquad (10)$$

It can be seen from equation [6] that the tendency to cleavage is enhanced by the presence of brittle particles at the grain boundaries in keeping with previous experimental data. Further grain size dependence of the fracture stress should be modified by the presence of brittle particles such that at fine grain sizes of the order of a few microns the criteria for propagation will become increasingly dependent on the carbide thickness t, rather than the grain size. There will be a further decrease in the grain size dependence of the fracture stress if all the dislocations in the pile up do not enter the crack [11]. Thus from expressions quoted earlier the grain size and the number of dislocations in the pile up are related by

$$na = \frac{(1-\nu)\ kl^{1/2}}{4\mu} \qquad (11)$$

so for $n' < n$ the grain size dependent term in expressions 6-10 will be decreased in magnitude relative to the carbide thickness term.

Experimental aspects

The predictions of the above model were examined in two respects. Firstly, the dependence of the fracture behaviour on the thickness of the grain boundary carbide and secondly the dependence of the fracture stress on grain size for a material containing coarse grain boundary carbides. Tensile notch bend and impact tests were performed on specimens of Armco iron with a composition, wt.%, 0·022C, 0·028Mn, 0·005P, 0·018S, 0·003Si, 0·052 Cu. The tensile tests were performed on specimens of 1 in gauge length and 0·115 in diameter and for notch bend and impact test specimens 6×6×44 mm with a centrally located Charpy V notch were used. Notch bend and tensile tests were performed at a crosshead speed of 0·2 in per min and a Zwick pendulum tester was used for the impact tests.

In order to examine the effect of boundary carbide size a comparison was made between furnace cooled specimens and specimens quenched from 725°C and aged for 8 hrs at 300°C. To obtain a suitable range of grain sizes the annealing treatments listed in Table 1 were used. All heat treatments were performed in an argon atmosphere and the specimens were furnace cooled to produce coarse grain boundary carbides.

The size dustribution of grain boundary carbides was established using optical and carbon replica techniques and fracture surfaces were examined using scanning electron microscopy.

Results

The sizes and distributions of grain boundary carbides are listed in Table 2. The quench aged specimens contained carbides with a thickness of about 0·3 microns and an interparticle spacing of 3 to 5 microns.

The results of the bend tests performed on specimens of different grain sizes are shown in Fig. 3 and the temperatures at which fracture coincided with general yield are tabulated in Table 3. At this temperature the maximum tensile stress below the notch is directly related to the tensile yield stress of the material by a factor [10]

$$R = \left(1 + \frac{\pi - \theta}{2}\right), \qquad (12)$$

for a notch angle θ and using the Tresca yield criterion. Thus by determining the yield stress in uniaxial tension at this temperature, the maximum tensile stress and hence the fracture stress can be calculated. Values of the yield stress at the relevant temperatures, −90, −102, −110, −115, −122 and −145°C were determined by performing tensile tests for a range of grain sizes and then interpolating the data to the particular grain size concerned. Values of k, the slope of the Hall-Petch equation, were also obtained from the yield stress data, and these are also tabulated in Table 2. Tests were also performed on specimens with a 90° notch angle and the results compared with those for specimens of the same grain size with a 45° notch, these are shown in Fig. 4.

The results of the impact tests in Fig. 5 show that the transition temperature of furnace cooled Armco iron specimens was reduced by approximately 60°C after quench ageing. A comparison of the fracture surfaces for the two heat treatments is shown in Fig. 6 where it can be seen that the cleavage facets in the material containing dispersed carbides contain numerous small steps and river lines. The spacing of these steps is of the order of three microns in good agreement with the spacing of the dispersed carbides revealed by transmission microscopy. The fracture surfaces of the furnace cooled specimens produced at various temperatures are shown in the sequence in Fig. 7, where there is evidence of an increasing amount of plastic deformation at grain boundaries as the testing temperature is increased from −196 to 56°C.

Discussion

For clarity the discussion is divided into three sections dealing with the effects of grain size, carbide distribution and crack propagation.

Grain size effects

In a tensile test when slip induced cleavage fracture occurs the amount of prior deformation is comparable to that experienced locally at the lower yield point. Thus even though the numerical value of the fracture stress, $4\ \mu\gamma 1^{-1/2}/k$, may be less than the yield stress a tensile specimen will not fracture until it has reached the yield stress. In contrast to this in notched bend test, once yield has been initiated from the root of a notch it will

spread continuously under an increasing longitudinal tensile stress and the specimen will fracture when the longitudinal tensile stress has been raised to the fracture stress. Knowing the degree of stress intensification that occurs at general yield it is possible to calculate the fracture stress when fracture coincides with general yield. The temperatures when this occurs and the corresponding fracture stresses are tabulated in Table 3 for specimens of different grain sizes. In order to utilize these results it must be assumed that the fracture stress is essentially independent of temperature over the range of temperatures examined. This has been found for a number of steels [12, 13] but in order to give some basis for this assumption in the present work specimens of constant grain size were tested with notch angles of 45° and 90°. The temperatures at which fracture was coincident with general yield were found to be −90°C and −110°C respectively (Fig. 4). The fracture stresses were calculated from the product of the stress intensification factor and the yield stress to be 61·5 kg.mm^{-2} at both temperatures. (In this instance and in the remainder of the discussion the values quoted for the fracture stress have been calculated using the Tresca criterion. In previous work [14] the authors have found this criterion to give more consistent results for small notch bend specimens than the Von Mises criterion). On the basis of this result the fracture stress was assumed to be insensitive to temperature over the range of temperatures examined.

The results for the variation of fracture stress with grain size are plotted in Fig. 8 where it can be seen that at finer grain sizes there is considerable deviation from the fracture stress grain size, $l^{-1/2}$, relationship as predicted by the model. A numerical fit to the experimental data can be made using a simpler version of equation (10).

$$p = \left(\frac{k^2 l}{4t^2} + \frac{4\mu\gamma}{t}\right)^{1/2} - \frac{k\, l^{1/2}}{2t}, \qquad (13)$$

and using the experimentally determined value for carbide size of 2·5 microns and Cottrell's [2] value for γ of 2×10^4 erg.cm^{-2}. As can be seen in Fig. 8, both the present results and Low's [15] results for a coarse grain sized 0·07% steel lie close to the derived curve.

Carbide distribution

The results quoted in Table 2 indicate that the fracture stress of 115 kg.mm for quench aged specimens with a grain size of 0·0373 mm was almost identical to the fracture stress of furnace cooled material with a grain size of 0·0145 mm. Thus reducing the carbide size has enabled the fracture strength to be preserved even though the grain size has increased. Although there were no measurements made of the fracture stress of furnace cooled specimens with a 0·0373 mm. grain size, a value can be obtained by interpolating the data in Fig. 8. The value obtained of 94 kg.mm^{-2} demonstrates the influence of carbide size on the fracture stress. Thus in this particular case the fracture stress has been increased by 21 kg.mm^{-2} by decreasing the carbide size from 2·5 to 0·3 microns. Using the above information and the results in Table 3 a comparison of the fracture behaviour of furnace cooled and quench aged materials can be made using equation 12 and substituting the appropriate values for p, k, l and t. Thus if $8\cdot3\times10^3$ kg.mm^{-2} is used for the shear modulus then a value of 2×10^4 erg.cm^{-2} is obtained for γ for both the furnace cooled and quench aged materials. Since these two heat treatments produced considerable differences in the carbide distribution it would appear that the effective surface energy involved in the initial process of propagating the crack from the carbide into the ferrite is unaffected by the dispersion of carbides in the quench aged material. However the total surface energy involved in crack propagation across the specimen may be dependent on carbide dispersion. Furthermore it cannot be assumed that the effective surface energy will be unaffected by all carbide dispersions. In the foregoing discussion it has been assumed that the grain boundary carbides exert a much greater influence on fracture behaviour than carbides dispersed within the grains. An alternative viewpoint has been proposed by Hahn and Rosenfield [11] who suggested that dispersed particles could increase the fracture stress by serving to reduce the effective pile up length from the grain diameter to the interparticle spacing. However previous experimental work [17] has shown that cementite particles dispersed within the grains serve to promote localized turbulent slip rather than crack initiation.

Crack propagation

The scanning electron microscopy of fracture surfaces has revealed two important topological features. Firstly the comparison of the fracture surfaces of materials in the furnace cooled and quench aged conditions indicates that dispersed particles serve to deflect the cleavage crack locally resulting in the formation of river lines or steps in the cleavage surface. Thus dispersed particles must serve to increase the total surface energy involved in the crack propagation process.

The regions of plastic deformation at grain boundaries on the fracture surfaces in Fig. 7 are indicative of a higher surface energy for crack propagation across grain boundaries in the transition temperature region. In tensile tests this same effect is responsible for the high incidence of non propagating grain size microcracks near the ductile brittle transition temperature [16, 3] and results in an increased total effective surface energy for crack propagation.

Summary and conclusions

A simple energy criterion is proposed for the propagation of a crack from a grain boundary carbide into the ferrite matrix under the combined action of the applied stress and the stresses at the tip of a pile up. The model has been tested by using notch bend tests to determine the condition where fracture occurs at general yield. The experimental results provide a limited confirmation of the model by demonstrating its ability to explain the effect of variations in both carbide thickness and grain size. It is shown that in the presence of grain boundary carbides the grain size dependence of the fracture stress deviates from the theories proposed by Cottrell and Petch. The results indicate that at very fine grain sizes of the order of a few microns the fracture stress will be determined predominantly by the thickness of the grain boundary carbides rather than the grain size. This may be of considerable practical significance in the technology of low alloy fine grain structural steels and thermal mechanically processed materials.

In addition scanning electron microscopy of fracture surfaces indicates that in the region of the transition temperature considerable plastic tearing may occur in the region of the grain boundary due to the difficulty of propagating a cleavage crack from one grain to the next. Also it would appear that dispersed second phase particles may greatly modify the topology of cleavage facets and thus raise the total surface energy required for crack propagation.

Acknowledgements

The authors wish to thank Dominion Foundries and Steel, Limited, of Hamilton for use of their scanning electron microscope, the Defence Research Board of Canada for research support and Mr R. Jaracowitz for assistance with the experiments.

References

1. PETCH, N. J. *Phil. Mag.*, vol. 3, p 1089, 1958.
2. COTTRELL, A. H. *Trans. AIME*, vol. 212, p. 192, 1958.
3. McMAHON, C. J. & COHEN, M. *Acta. Met.*, vol. 13, p. 591, 1965.
4. GELL, M. & WORTHINGTON, P. J. *Acta Met.*, vol. 14, p. 1265, 1966.
5. ALLEN, N. P., REES, W. P., HOPKINS, B. E. & TIPLER, H. R. *JISI*, vol. 174, p. 108, 1953.
6. STROH, A. N. *Advances in Physics*, vol. 6, p. 418, 1957.
7. SMITH, E. *Acta Met.*, vol. 14, p. 985, 1966
8. SMITH, E. *Physical Basis Yield and Fracture*, Conf. Proc., Oxford, p. 36, 1966.
9. STROH, A. N. *Proc. Roy. Soc.*, vol. 223A, p. 404, 1954.
10. GREEN, A. P. & HUNDY, B. B. *J. Mech. Physics Solids*, vol. 4, p. 128, 1956.
11. HAHN, G. T. & ROSENFIELD, A. R. *Acta. Met.*, vol. 14, p. 1815, 1966.
12. KNOTT, J. F. *JISI*, vol. 204, p. 104, 1966.
13. OATES, G. *JISI*, vol. 206, p. 930, 1968.

14. ALMOND, E. & EMBURY, J. D. *Met. Science Journal*, vol. 2, p. 194, 1968.
15. LOW, J. R. Jr. 'Iron and Its Dilute Solid Solutions', Wiley, New York, p. 255, 1963.
16. HAHN, G. T., OWEN, W. S., AVERBACH, B. L. & COHEN, M. 'Fracture', Wiley, New York, p. 91, 1959.
17. ALMOND, E., TIMBRES, D. H. & EMBURY, J. D. *Can. Met. Quart.*, (in the press).

Table 1
The heat treatments used to obtain the various grain sizes

Heat treatment	*grain size, mm*
Reduced 25% by cold swageing, annealed 725°C for 1 hr.	0·1045
Annealed at 725°C for 1 hr., 25% reduction, annealed 725°C for 5 hr.	0·0234
Annealed at 725°C for 1 hr., 25% reduction, annealed 750°C for 12 hr.	0·0230
Reduced 25% by cold swageing, annealed 925°C for 1 hr.	0·0860
As received, annealed 925°C for 1 hr. and 1200°C for 3 hr.	0·1680
Annealed at 725°C for 1 hr., 25% reduction, annealed 725°C for 15 hrs.	0·0370

Table 2
Grain boundary carbide distribution per hundred carbides

Grain size	*Thickness (microns)*					
(mm)	<1	1	1·5	2·0	2·5	>2·5
	Carbide					
0·0145	9	23	24	24	15	5
0·0230	6	35	23	24	11	1
0·0234	14	37	17	13	15	4
0·0860	7	29	29	22	11	2
0·1680	13	22	36	17	11	1

Table 3

Values of the yield stress, the fracture stress and k, at the temperatures when fracture coincides with general yield. The values of the yield stresses and k were obtained from uniaxial tensile tests.

	Grain size mm	Transition temperature °C	Yield stress kg.mm^{-2}	Fracture stress kg.mm^{-2} Tresca	Fracture stress kg.mm^{-2} Von Mises	k kg. mm$^{-3/2}$
Furnace cooled, 45° notch	0·168	−90	28·2	61·4	72·4	2·43
,,	0·086	−102	33·0	71·8	84·7	2·35
,,	0·0234	−110	44·5	97·0	114·3	2·45
,,	0·0230	−115	47·0	102·3	120·8	2·40
,,	0·0145	−122	52·4	114·2	134·7	2·44
Furnace cooled, 90° notch	0·168	−110	34·4	61·8	70·8	2·45
Quench aged 45° notch	0·037	−145	52·9	115·2	136·0	2·80

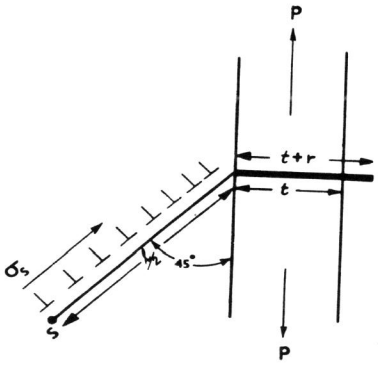

Fig. 1. Schematic representation of a crack in a carbide being assisted in propagation by the applied normal stress and the stresses due to the slip band.

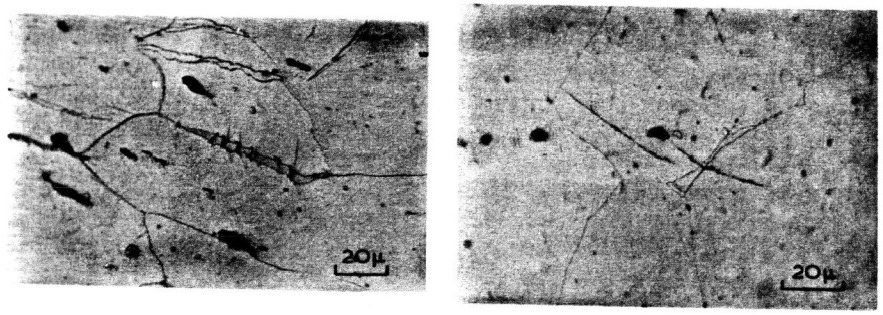

Fig. 2

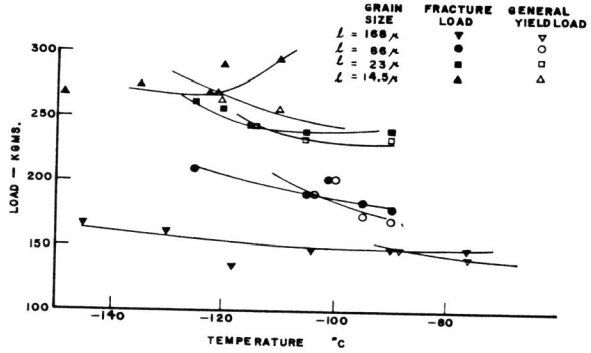

Fig. 3. Fracture load and general yield load of notch bend Armco iron specimens with differenc grain sizes as a function of temperature.

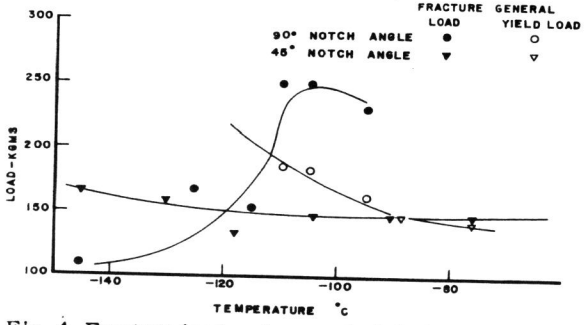

Fig. 4. Fracture load and general yield load of notch bend Armco iron specimens with 45° and 90° notch angles as a function of temperature.

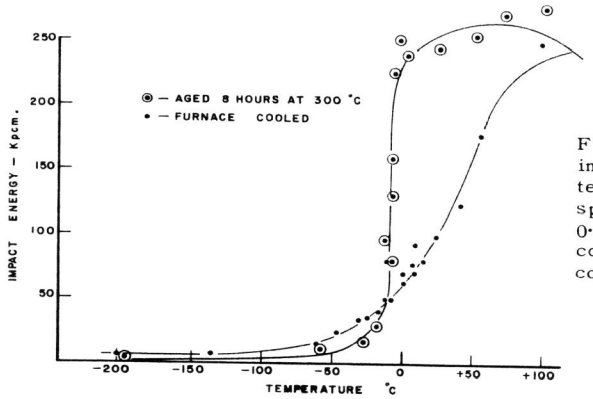

Fig. 5. The variation of impact energy with testing temperature for Armco iron specimens of grain size 0·03 mm. in the furnace cooled and quench aged condition.

Fig. 6. The fracture surfaces of (a) a furnace cooled impact specimen and (b) a quench aged impact specimen both tested at –196°C, showing the increased density of river lines after quench ageing.

Fig. 8. The present results and the results of Low [8] for the variation of fracture stress with grain size. The solid line is the curve of the equation

$$p = \left(\frac{k^2 l}{4t^2} + \frac{4\mu\gamma}{l}\right)^{1/2} - \frac{k\, l^{1/2}}{2t}$$

obtained by using values of 2·5 microns for t, 2·41 kg.mm$^{-3/2}$ for k, 2×10^4 erg.cm^{-2} for γ and $8{\cdot}3 \times 10^3$ kg.mm^{-2} for μ.

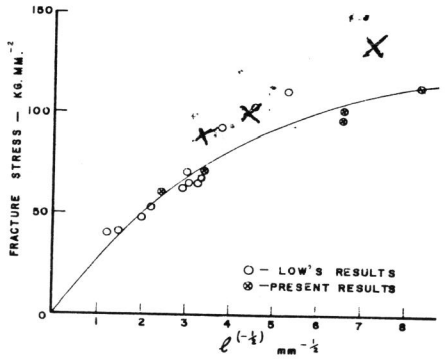

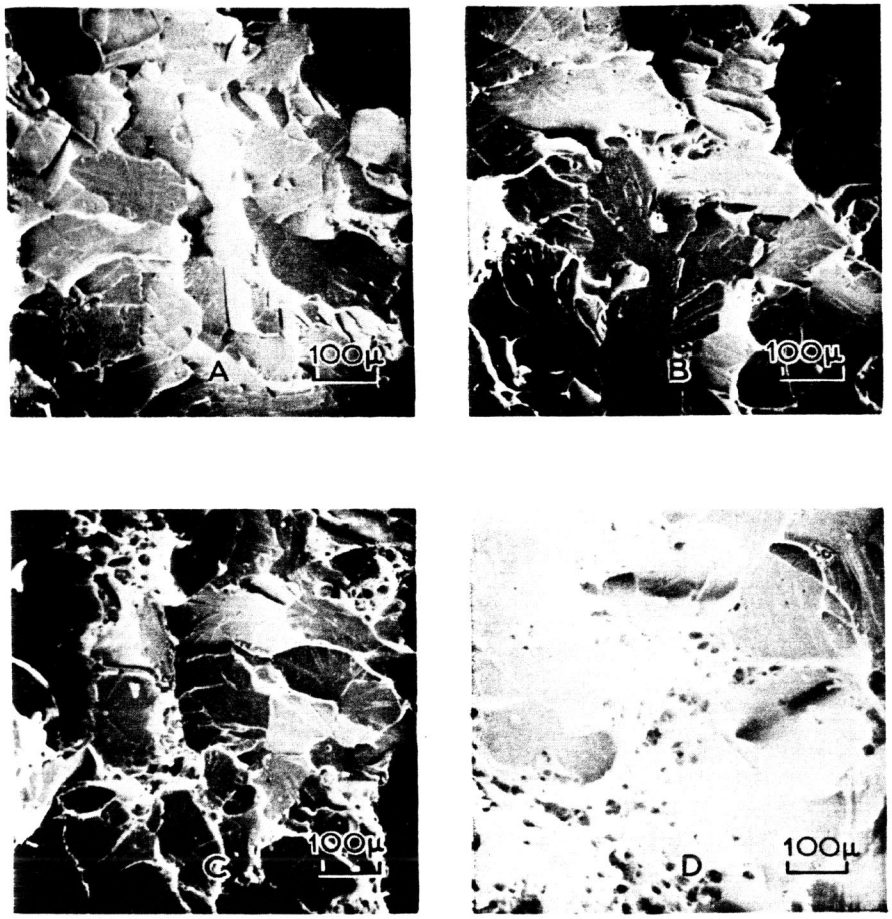

Fig. 7. The fracture surfaces of furnace cooled impact specimens tested at (a) –196°C, (b) –65°C (c) –18°C and (d) +56°C.